Mechanisms of Economic Decisions under Sequential Offers

Authors: Sébastien Ballesta[a,¶] and Camillo Padoa-Schioppa[a,b,c]

Affiliations: [a]Department of Neuroscience, [b]Department of Economics and [c]Department of Biomedical Engineering, Washington University in St. Louis, St. Louis, MO, 63110, USA.

¶ Present address: Laboratoire de Neurosciences Cognitives et Adaptatives, Strasbourg, France. Centre de Primatologie de l'Université de Strasbourg, Niederhausbergen, France

Manuscript information: 160 words in abstract, 4690 words in main text, 7 figures, 1 table, supplementary information in separate file.

Keywords: neuroeconomics, orbitofrontal cortex, mutual inhibition, circuit inhibition, monkey, neurophysiology

Correspondence: Camillo Padoa-Schioppa, Department of Neuroscience, Washington University in St Louis, Tel: 314-747-2253, Email: *camillo@wustl.edu*

Acknowledgments: We thank H. Schoknecht for help with animal training and E. Bromberg-Martin, K. Conen, A. Jezzini, I. Monosov, W. Shi and M. Zhang for comments on the manuscript. This research was supported by the National Institutes of Health (grant number R01-DA032758 to CPS).

Conflict of interest: None

Abstract

Binary choices between goods are thought to take place in orbitofrontal cortex (OFC). However, current notions emerged mostly from studies where two offers were presented simultaneously. Other work suggested that choices under sequential offers rely on fundamentally different mechanisms. Here we recorded from the OFC of macaques choosing between two juices offered sequentially. Analyzing neuronal responses across time windows, we discovered different groups of neurons that closely resemble those identified under simultaneous offers, suggesting that decisions in the two modalities are formed in the same neural circuit. Building on this result, we examined five hypotheses on the decision mechanisms. OFC neurons encoded goods and values in a juice-based representation (labeled lines). Contrary to previous assessments, decisions did not involve mutual inhibition between pools of offer value cells. Instead, decisions involved mechanisms of circuit inhibition, whereby each offer value indirectly inhibited neurons encoding the opposite choice outcome. These results reconcile seemingly disparate findings and provide a unitary account for economic decisions.

Introduction

Recent years have witnessed enormous progress in understanding the mechanisms underlying economic choices. This behavior is thought to involve two mental stages – values are assigned to the available options, and a decision is made by comparing values. Evidence from clinical data[1-3], functional imaging[4,5], neurophysiology[6-8] and lesion studies[9-11] links economic decisions to the orbitofrontal cortex (OFC). Neurophysiology experiments in which monkeys chose between different juices offered in variable amounts identified different groups of cells encoding the value of individual options (*offer value*), the binary choice outcome (*chosen juice*) and the *chosen value*[12,13]. These variables capture both the input and the output of the decision process, suggesting that these groups of cells constitute the building blocks of a decision circuit[8,14]. Supporting this proposal, trial-to-trial variability in each group of neurons correlates with choice variability[13,15]. Furthermore, neuronal dynamics in OFC during economic decisions reflect an internal deliberation[16]. Complementing these experimental findings, theoretical work showed that neural networks whose units match the cell groups identified in OFC can generate binary decisions (**Fig.1ab**)[17-21]. Collectively, these results appear to lay the foundations for a satisfactory understanding of the mechanisms underlying economic decisions. In other words, while many aspects of the circuit depicted in **Fig.1b** need to be elucidated, the basic scheme would seem to be in place. A fundamental limitation of this assessment is the fact that the vast majority of previous studies examined choices between goods offered simultaneously. Yet, in many real-life decisions, offers appear sequentially. Moreover, in natural settings, subjects often shift their gaze, and thus their mental focus, back and forth between options. Current models for choices under simultaneous offers do not account for choices under sequential offers. More precisely, current models can be modified to do so, but there are multiple ways in which such modification may be done (see below).

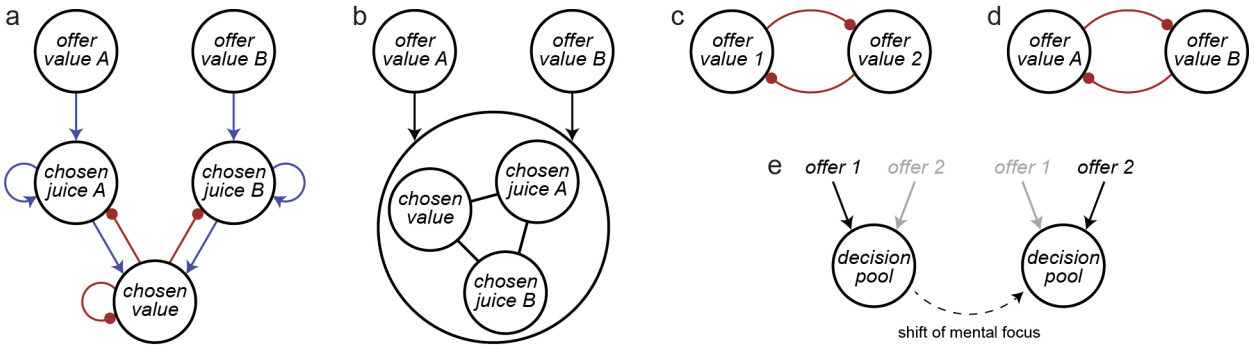

Figure 1. Decision models. **(a)** Biophysically realistic network based on recurrent excitation and pooled inhibition. Blue and red indicate excitation and inhibition, respectively. This model, originally proposed for perceptual decisions [38], captures well the activity of different groups of neurons in OFC during choices under sequential offers [21]. **(b)** General scheme common to multiple models of decisions under simultaneous offers [20-24]. In essence, two pools of offer value cells provide the primary input to a neural circuit composed of chosen juice cells and chosen value cells, where decisions are made. The model in panel (a) is one example of the general model shown in panel (b). **(c)** Mutual inhibition at the level of offer values. In this model, decisions take place through mutual inhibition of two populations of neurons encoding the two offer values. This version of the model assumes that options are defined by the sequential order (1 and 2; order-based representation). **(d)** Mutual inhibition in juice-based representation. The mode is similar (d), except that options are defined by the juice type (A and B). **(e)** Decisions without labeled lines. In this model, the same neural pool examines sequentially the two offers and makes independent accept/reject decisions. Models (c) and (e) are from Hayden and Moreno-Bote (2018) [33].

Importantly, some previous studies did examine choices under sequential offers[22-28]. Unfortunately, their findings are often hard to compare with those summarized above, largely because data analyses did not address seemingly crucial questions. Indeed, most studies of choices under sequential offers did not attempt to identify different groups of neurons that might play different roles in the decision process[22-27,29]. Furthermore, most analyses assumed that neurons in OFC (or other areas) represent options and values in the reference frame defined by the sequential order, and did not test alternative reference frames[23-28]. Failure to consider alternative reference frames can explain negative results obtained when categorization analyses were attempted[28]. In some cases, major conclusions were drawn from negative results[25]. Last but not least, data sets were relatively small and perhaps insufficient to assess the presence of different cell groups[23-27]. Despite these limitations, previous work on choices under sequential offers put forth two testable hypotheses. First, some studies proposed that decisions take place through mechanisms of mutual inhibition between pools of offer value cells (**Fig.1cd**)[23,24]. Second, other studies challenged the notion that neurons in the decision circuit are associated with individual offers (i.e., the idea of "labeled lines")[26,27,30]. Specifically, it was proposed that choices – including binary choices – are processed as sequences of accept/reject decisions[30]. In this view, each offer value is separately compared to an internal benchmark; the decision circuit is constituted of a single pool of neurons that sequentially evaluates and accepts or rejects different options, without a competition between different groups of cells (**Fig.1e**)[30]. Both proposals are radically in contrast with the scheme depicted in **Fig.1b**. As a possible reconciliation, some authors speculated that decisions under sequential versus simultaneous offers rely on separate neural circuits[24,30-32]. This last hypothesis, however, has not been tested.

To shed light on the mechanisms of choices under sequential offers, we recorded from a large population of OFC neurons while monkeys chose between two juices offered sequentially and in variable amounts. We analyzed firing rates with approaches similar to those previously used for choices under simultaneous offers[12,13]. Most task-related neurons encoded the value or identity of one particular juice type. Their activity in any time window depended on the presentation order. However, an analysis of neuronal responses across time windows revealed the presence of different groups of cells seemingly corresponding to the groups of cells previously identified under simultaneous offers[12,13]. This result suggested that decisions in the two modalities may be formed in the same neural circuit. Building on this observation, we tested five hypotheses on the decision mechanisms. Our data confuted the notion of a single neuronal pool (**Fig.1e**). They were also inconsistent with mutual inhibition between pools of offer value cells (**Fig.1cd**). Under sequential offers, the first offer value affects the decision process taking place after a delay. One possibility is that a population of *offer value* cells maintains a sustained working-memory representation of the first offer value until when the second offer is presented. Our data did not support this proposal. In contrast, our data pointed to a mechanism of circuit inhibition, whereby neurons encoding the first offer value (input layer) indirectly inhibit neurons representing the second choice outcome (output layer). This inhibited state affects the decision upon presentation of the second offer.

Results

In the experiments, monkeys chose between two juices offered in variable amounts. The two juices were labeled A and B, with A preferred. The two offers were presented centrally and sequentially (**Fig.2a**). The terms "offer1" and "offer2" refer to the first and second offer, independently of the juice type and amount. After a delay following offer2, two targets appeared on the two sides of the fixation point, and monkeys indicated their choice with a saccade. For each pair of juice quantities, the sequential order of the two offers varied pseudo-randomly. We

were specifically interested in binary choices that require evaluating both offers, with decisions taking place after offer2. In principle, if the value of offer1 is very low or very high, the animal could finalize its decision before offer2. To limit this issue, we designed offer types such that in most trials the animal had to wait for offer2 before making a decision (**Fig.2b**). In each session, the choice pattern was analyzed with a logistic regression, from which we derived a measure for the relative value of the juices (see Methods).

Encoded variables

We recorded the activity of 1267 cells from the OFC of two animals. We examined firing rates in eight 0.5 s time windows aligned with different behavioral events (pre-offer, post-offer1, inter-offer, post-offer2, offers off, fixation off, pre-juice, post-juice; see Methods). Trials in which juice A was offered first and trials in which juice B was offered first were referred to as "AB trials" and "BA trials", respectively. An "offer type" was defined by two juice quantities in given order (e.g., [1A:3B] or [3B:1A]); a "trial type" was defined by an offer type and a choice (e.g., [1A:3B, B]); and a "neuronal response" was defined as the activity of one cell in one time window as a function of the trial type. We submitted each neuronal response to an ANOVA (factor: trial type, $p<0.001$). Neurons passing the criterion in at least one time window were identified as "task-related" and underwent further analysis.

Considering all 8 time windows, 612/1267 (48%) cells were task-related (**Table S1**). Restricting the analysis to the 3 primary time windows (post-offer1, post-offer2, post-juice), 538/1267 (42%) cells were task-related. In a first assessment, many neurons seemed to present different patterns of firing rates in AB versus BA trials. For example, **Fig.3ab** illustrates the activity of one cell (post-offer1 time window) plotted against variable *offer value 1*. In AB trials, the firing rate increased as a function of the offered value (the cell seemed to encode the *offer value A*). In contrast, in BA trials, the cell was untuned. Such cases were frequent. However, firing rates in the two sets of trials were usually not unrelated. For example, for the cell in **Fig.3b**, the firing rates recorded in BA trials were close to what would be expected if juice A had been offered in quantity 0. In other words, we could define a single variable *offer value A | AB* (= *offer value A* in

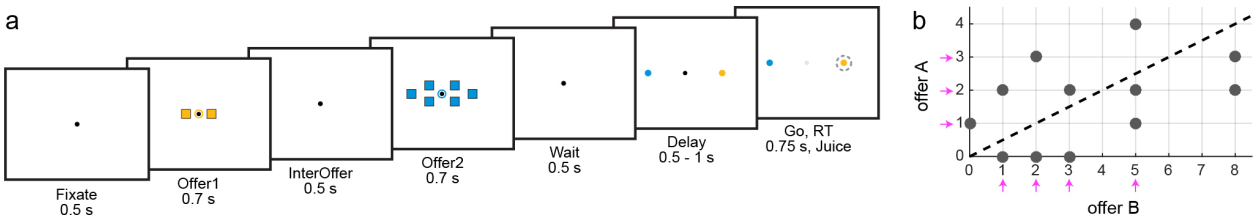

Figure 2. Experimental design. **(a)** The trial started with the animal fixating a center dot. Two offers were presented centrally and sequentially. The color and number of squares represented the juice type and the juice quantity, respectively. In the trial depicted here, the animal chose between two drops of grape juice and six drops of peppermint tea. The second offer was followed by a wait time, after which two saccade targets associated with the two juices appeared on the monitor. After a randomly variable delay, the center fixation point disappeared (go signal), and the animal indicated its choice with a saccade. For each pair of quantities, the sequential order of the offers and the left/right positions of the saccade targets varied pseudo-randomly. **(b)** Offer types for a representative session. The y-axis and x-axis represent quantities of juices A and B offered, gray circles indicate offer types included in the session, and the dotted line (indifference line) captures the relative value of the two juices ($\rho = 2$). For offers types above (below) the indifference line, the animal usually chose juice A (juice B). Pink arrows indicate juice quantities that, if presented as offer1, prevented the animal from finalizing its decision before offer2 (because, for given offer1, choices were split almost equally between the two juices).

AB trials and = 0 in BA trials) that explained the whole neuronal response. More formally, assuming linear tuning, any neuronal response can be written as:

$$r = (a_0 + a_1\ var1)\ \delta_{order,AB} + (a_2 + a_3\ var2)\ \delta_{order,BA} \quad (1)$$

where r is the firing rate, *var1* and *var2* are two variables, $\delta_{order,XY} = 1$ if the order is XY and 0 otherwise, and a_0 ... a_3 are regression coefficients. In the general case, *var1* and *var2* can be

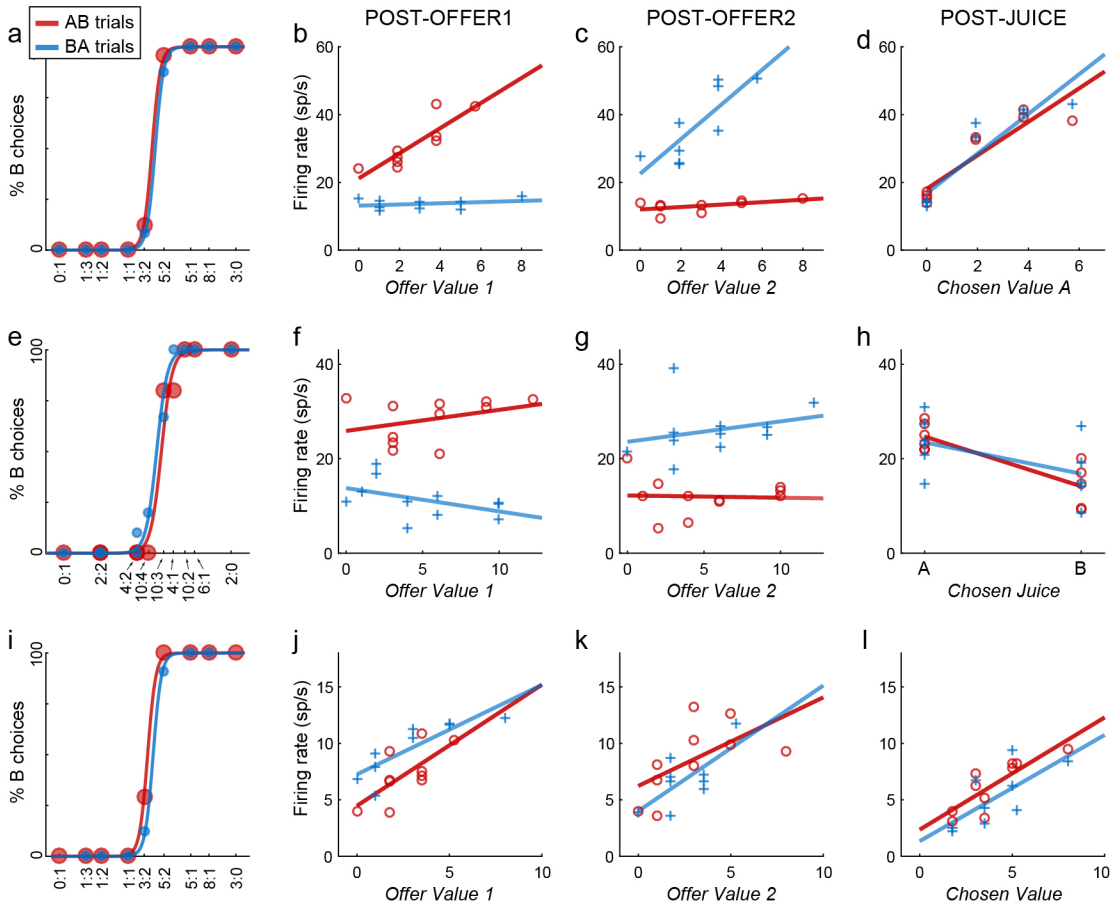

Figure 3. Example cells. Each row illustrates the activity of one neuron. For each cell, the four panels illustrate the behavior and the firing rates in post-offer1, post-offer2 and post-juice time windows. Red and blue colors always refer to AB trials and BA trials, respectively. **(a)** Example cell 1, choice pattern. The percent of B choices is plotted against the log quantity ratio. Sigmoid curves are from a logistic regression (Eq.3). **(b)** Activity in post-offer1. Each data point represents one trial type (with firing rate averaged across ~15 trials). Lines were obtained from linear regressions. When juice A was offered (AB trials, red), firing rates increased as a function of the offer value; when juice B was offered (BA trials, blue), firing rates were always low. This neuronal response can be described as encoding the variable offer value A | AB. **(c-d)** In other time windows, this cell encoded variables offer value A | BA (panel c) and chosen value A (panel d). **(e-h)** Example cell 2. In each time windows the activity of this cell was roughly binary. In the post-offer1 time window, the activity was high in AB trials (red) and low in BA trials (blue) (variable AB | BA; panel f). In the post-offer2 time window, the activity was high in BA trials and low in AB trials (variable – AB | BA; panel g). In the post-juice time window, the activity was high when the animal chose juice A and low when it chose juice B (variable chosen juice A; panel h). **(i-l)** Example cell 3. In the three time windows, this neuron encoded variables offer value 1, offer value 2 and chosen value.

any two variables and a_0 ... a_3 are independent of one another. In contrast, for the vast majority of neuronal responses, we could define a single variable encoded in both sets of trials with the same coefficients, such that **Eq.1** reduced to:

$$r = a_0 + a_1\ var1 \qquad (2)$$

A description of firing rates according to **Eq.2** greatly simplified our understanding of neuronal responses in OFC.

We considered a large number of variables conceivably encoded in OFC. These included a variable indicating the presentation order (*AB* | *BA*), eight variables associated with individual offers (*offer value A*, *offer value A* | *AB*, *offer value A* | *BA*, *offer value 1*, *offer value 2*, etc.),

a

	Offer value A	Offer value A | AB	Offer value A | BA	Offer value B	Offer value B | AB	Offer value B | BA	Offer value 1	Offer value 2	Other value	Chosen value	Chosen value A	Chosen value B	Chosen juice	AB|BA	Chosen order	Value diff (ch-oth)	Value diff (1-2)	Value diff (A-B)
Post-offer1	90	190	183	112	164	233	193	57	125	104	22	15	6	222	48	10	132	10
Inter-offers	52	115	118	53	95	133	109	30	57	54	21	17	5	136	33	10	68	13
Post-offer2	97	201	211	99	251	197	93	210	107	111	31	44	20	251	106	21	174	22
Offers off	85	92	100	98	126	93	72	131	81	114	57	62	39	110	49	37	64	43
Fix off	41	8	10	45	17	10	28	27	25	43	49	53	55	1	0	22	3	25
Pre-juice	79	9	17	78	25	17	32	39	38	73	122	129	142	1	3	42	0	40
Post-juice	100	9	24	98	28	19	57	66	64	99	129	128	145	0	0	51	1	47

b

	Offer value A	Offer value A | AB	Offer value A | BA	Offer value B	Offer value B | AB	Offer value B | BA	Offer value 1	Offer value 2	Other value	Chosen value	Chosen value A	Chosen value B	Chosen juice	AB|BA	Chosen order	Value diff (ch-oth)	Value diff (1-2)	Value diff (A-B)
Post-offer1	4	48	6	3	5	68	93	0	5	3	1	0	1	102	2	0	0	1
Inter-offers	7	20	3	4	1	33	44	0	5	6	1	0	2	87	0	2	5	1
Post-offer2	5	15	57	3	64	12	9	78	16	6	2	3	2	107	7	2	22	2
Offers off	11	10	23	10	43	8	12	41	10	20	8	5	7	35	7	2	6	2
Fix off	8	1	0	8	0	1	3	1	4	10	4	7	34	0	0	1	1	1
Pre-juice	5	0	0	11	2	1	2	2	1	10	17	18	91	0	0	2	0	2
Post-juice	12	0	0	14	2	1	0	3	3	24	26	23	76	0	0	5	0	0

Figure 4. Encoded variables, population analysis. **(a)** Each response passing the ANOVA criterion was regressed on each of the 18 variables. If the regression slope differed significantly from zero ($p<0.05$), the variable was said to explain the response. Each response could be explained by >1 variable. Numbers in this panel indicate the number of responses explained by each variable in each time window. For example, variable offer value A explained 90 responses in the post-offer1 time window. The background image represents the same numbers in gray scale. **(b)** For each response, we identified the variable that provided the best fit (non-zero slope, highest R2). In this panel, numbers indicate responses best explained by each variable in each time window. For example, in the post-offer1 time window, variable offer value A provided the best explanation for 4 responses. The background image represents the same numbers in gray scale. Notably, different sets of variables explained a disproportionately high number of responses in different time windows. The same cell was often explained by different variables in different time windows, and specific patterns were most frequent. For the analysis of sequences, we focused on time windows post-offer1, post-offer2 and post-juice.

variables capturing the binary choice outcome (*chosen juice*, *chosen order*), variables associated with the chosen value (*chosen value*, *chosen value A*, etc.), and variables representing the value difference (*value diff (A–B)*, etc.). In total, we examined 18 variables (see Methods, **Table S2**, **Fig.S1**). Each response was separately regressed on each variable. If the regression slope differed significantly from zero ($p<0.05$), we said that the variable "explained" the response, and we noted the slope sign and the R^2. Of the 1751 responses passing the ANOVA criterion, 1671 (95%) were explained by at least one of the 18 variables. **Fig.4** provides a population summary of the variables encoded in different time windows.

Neuronal classification

Studies of choices under simultaneous offers found that OFC neurons encoded the same variable across time windows[13,33]. This property was important because it allowed to identify distinct groups of neurons. In contrast, most neurons recorded here appeared to encode different variables in different time windows. **Fig.3a-d** illustrates one example. During the post-offer1, the cell encoded the variable *offer value A | AB* (**Fig.3b**); during the post-offer2, the cell encoded the variable *offer value A | BA* (**Fig.3c**); during the post-juice, the cell encoded the

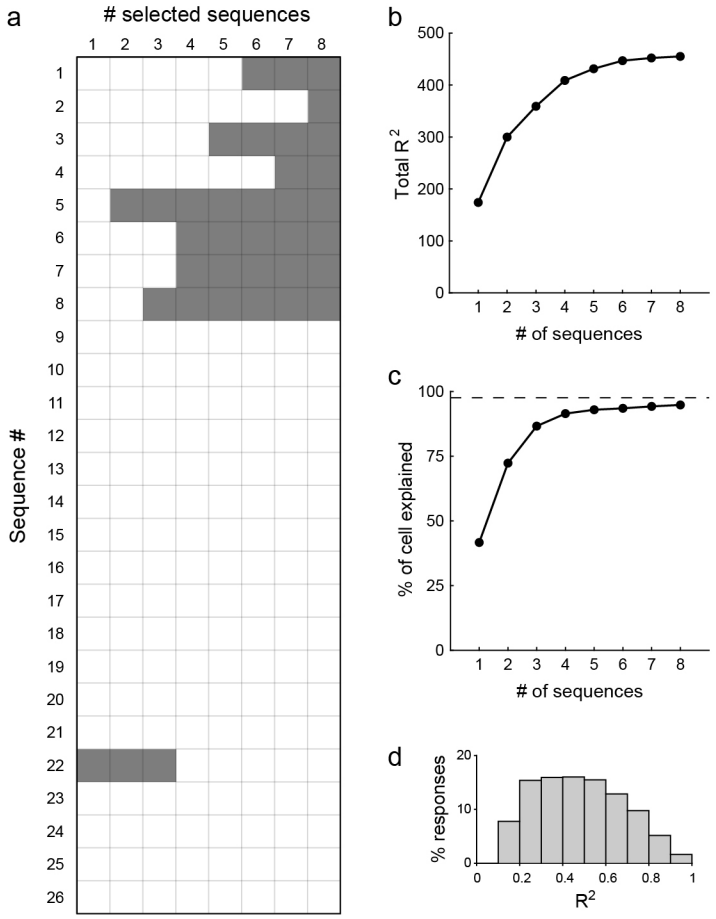

Figure 5. Sequence selection analysis. Given the high number of possible sequences, an exhaustive search for the best subset of k = 1,2,... sequences was prohibitive. Thus we restricted the analysis to sequences that provided the best explanation for ≥3 cells (26 sequences total). Then for k = 1,2,.. we selected the best subset of k sequences based on the total R2 (Methods). **(a)** Sequences selected at each iteration. Sequence numbers 1... 26 (y-axis) correspond to those detailed in Table S3. For each iteration (x-axis), selected sequences are indicated with a gray shade. Notably, in addition to the final 8 sequences, only one other sequence (#22) is ever selected. **(b)** Total R2. The x-axis represents the number of sequences; the y-axis represents the total R2 (summed across time windows and across cells). **(c)** Percent of explained cells. In this panel, 100% corresponds to the number of cells that passed the ANOVA in at least one time window (task-related cells, N=538). The dotted line indicates the percent of cells explained by all 46,656 sequences (N=525, 98%). The best subset of 8 sequences explained 510 cells (i.e., 95% of task-related cells and 97% of cells explained by all 46,656 sequences). Of note, these 8 sequences explained all of the cells explained by the 26 sequences included in the analysis. **(d)** Distribution of R2 across cells and across variables. For each classified cell (N=510), we considered the time windows that passed the ANOVA, and the R2 obtained from the corresponding variable. The panel illustrates the resulting distribution. Across the population, we measured mean(R2) = 0.48 ± 0.06 (mean ± SEM).

chosen value A (**Fig.3d**). Another example is shown in **Fig.3e-h**. In the same three time windows, this neuron encoded variables *AB | BA*, *– AB | BA*, and *chosen juice A*. Finally, in the same time windows, the cell in **Fig.3i-l** encoded variables *offer value 1*, *offer value 2*, and *chosen value*. At first, this variability seemed puzzling. However, the variables encoded by a given cell in different time windows were often closely related. For example, consider the neuron in **Fig.3a-d**. During post-offer1 and post-offer2, the cell encoded the offer value A whenever A was on the monitor. After juice delivery, the cell encoded the value of juice A whenever juice A was delivered. Now consider the cell in **Fig.3e-h**. The activity of this neuron was roughly binary in every time window. During post-offer1 and post-offer2, the activity was high whenever juice A was on the monitor. During post-juice, the activity was high whenever juice A was delivered. Finally, consider the cell in **Fig.3i-l**. During post-offer1 and post-offer2, the cell encoded the value of the good present on the monitor. During post-juice, the cell encoded the value chosen (and received) by the animal.

Following these observations, we sought to assess whether OFC neurons typically encode the same *sequence* of variables across time windows. For this analysis, we focused on the 3 primary time windows (post-offer1, post-offer2, post-juice). Considering 18 variables, 2 signs of the encoding and 3 time windows, there were 46,656 possible sequences of variables. Our goal was to assess whether a small subset of sequences could account for the entire data set. In principle, one could conduct an exhaustive analysis considering all the subsets of k = 1,2,3... sequences. For each k, one could identify the best subset as that with the highest explanatory power. Unfortunately, with so many possible sequences, an exhaustive search was not feasible. However, we noticed that sequences providing the best explanation for at least some neuron were relatively few. Thus we focused on 26 sequences that best explained at least 3 cells (**Table S3**), and we conducted an exhaustive search (see Methods). Remarkably, we found that a small number sequences accounted for most of the population. Specifically, the best subset of 8 sequences explained 510/538 (95%) of task-related cells (**Fig.5**, **Table 1**).

Seq.	post-offer1	post-offer2	post-juice	# cells	Label
#1	*offer value A | AB +*	*offer value A | BA +*	*chosen value A +*	65	*offer value A +*
#2	*offer value A | AB –*	*offer value A | BA –*	*chosen value A –*	24	*offer value A –*
#3	*offer value B | BA +*	*offer value B | AB +*	*chosen value B +*	85	*offer value B +*
#4	*offer value B | BA –*	*offer value B | AB –*	*chosen value B –*	31	*offer value B –*
#5	*AB | BA +*	*AB | BA –*	*chosen juice +*	71	*chosen juice A*
#6	*AB | BA –*	*AB | BA +*	*chosen juice –*	100	*chosen juice B*
#7	*offer value1 +*	*offer value2 +*	*chosen value +*	56	*chosen value +*
#8	*offer value1 –*	*offer value2 –*	*chosen value –*	78	*chosen value –*

Table 1. Results of sequence analysis and cell classification. Each neuron was then assigned to one of the selected sequences based on the sequence R^2. In the table, the leftmost column indicates the sequence number; columns 2-4 indicate the variables encoded in each of the three time windows; column 5 indicates the number of cells assigned to the sequence; the last column indicates the label used to refer to each sequence. In some of the subsequent analyses, we pooled cells from sequences #1 and #3 (*offer value +*), sequences #2 and #4 (*offer value –*), and sequences #5 and #6 (*chosen juice*).

Inspection of **Table 1** reveals that the sequences selected by the best-subset procedure may be divided in 3 groups. Moreover, there seems to be a correspondence between the groups of cells found here and those previously identified during decisions under simultaneous offers[12,13].

Specifically, sequences #1, #2, #3 and #4 resemble the cell in **Fig.3a-d** (considering two juices and two signs of the encoding); these neurons seem analogous to *offer value* cells identified previously. Sequences #5 and #6 resemble the cell in **Fig.3e-h**; these neurons seem analogous to *chosen juice* cells identified previously. Sequences #7 and #8 resemble the cell in **Fig.3i-l**. These neurons are less easy to interpret. However, there is a possible analogy with *chosen value* cells identified previously, in the sense that these neurons encode the value of either juice, provided that the animal focuses on it. The understanding in terms of mental focus is a valid interpretation of *chosen value* cells in our previous studies. Future work will test this correspondence more directly (see Discussion). In the following, we tentatively refer to these groups of cells using the labels *offer value*, *chosen juice*, and *chosen value*.

Decision mechanisms

Our aim was to understand how the cell groups detailed in **Table 1** support decisions. We specifically examined five hypotheses.

Hypothesis 1 (H1): Single pool. It has been proposed that decisions under sequential offers are processed by a single pool of neurons, as sequences of accept/reject decisions, without labeled lines[26,30] (**Fig.1e**). However, as discussed above, the majority (70%) of task-related cells in our data set were associated with a particular juice, either A or B (sequences #1 to #6). Moreover, these neurons responded differently to offer1 and offer2. These observations are inconsistent with the idea of a single pool and demonstrate the presence of labeled lines. One objection might be that perhaps neuronal activity in OFC is completely unrelated to decisions under sequential offers. However, in a different study we found that electrical stimulation of OFC interferes with choices under either simultaneous or sequential offers (Ballesta et al., in preparation).

Hypothesis 2 (H2): Mutual inhibition in order-based representation. Several studies examined choices under sequential offers and proposed that decisions take place through mutual inhibition at the level of offer value cells (**Fig.1c**)[23,24,26,27]. In those experiments, offers available for choice had some distinctive characteristic represented by a visual trait. For example, in one choice task, the two offers were associated with different reward magnitudes represented by different colors[23,24]. The analysis focused on the post-offer2 time window. Neuronal responses were normalized and regressed against variables *offer value 1* and *offer value 2*, and each term provided a beta coefficient. The key finding was that the two beta coefficients were negatively correlated across the population (beta anticorrelation). This observation was taken as evidence that decisions relied on mutual inhibition at the level of offer values. However, that conclusion was unwarranted because beta anticorrelation may hold regardless of the decision mechanisms. We detail this argument in the **Supplementary Note**. In essence, previous studies assumed that the neuronal representation of goods and values was order-based. However, this crucial assumption was not tested, and the choice tasks also afforded a color-based representation. Furthermore, goods defined by the color were offered in different value ranges. In these conditions, neurons encoding the identity or value of individual goods necessarily present beta anticorrelation, independent of the decision mechanisms (**Fig.S3**). Mindful of this issue, we examined beta coefficients in our data set. In neurons recorded with unequal value ranges, we replicated the results of previous studies[23-27]. However, once differences in value range were controlled for, beta coefficients did not present any positive or negative correlation (**Fig.S4**). In other words, we did not find any support for H2.

Hypothesis 3 (H3): Mutual inhibition in juice-based representation. In principle, decisions may entail mutual inhibition between pools of offer value cells associated with different juice types (**Fig.1d**). If so, when the decision takes place, the activity of neurons directly involved in the decision should reflect the difference between the two offer values. Contrary to this prediction,

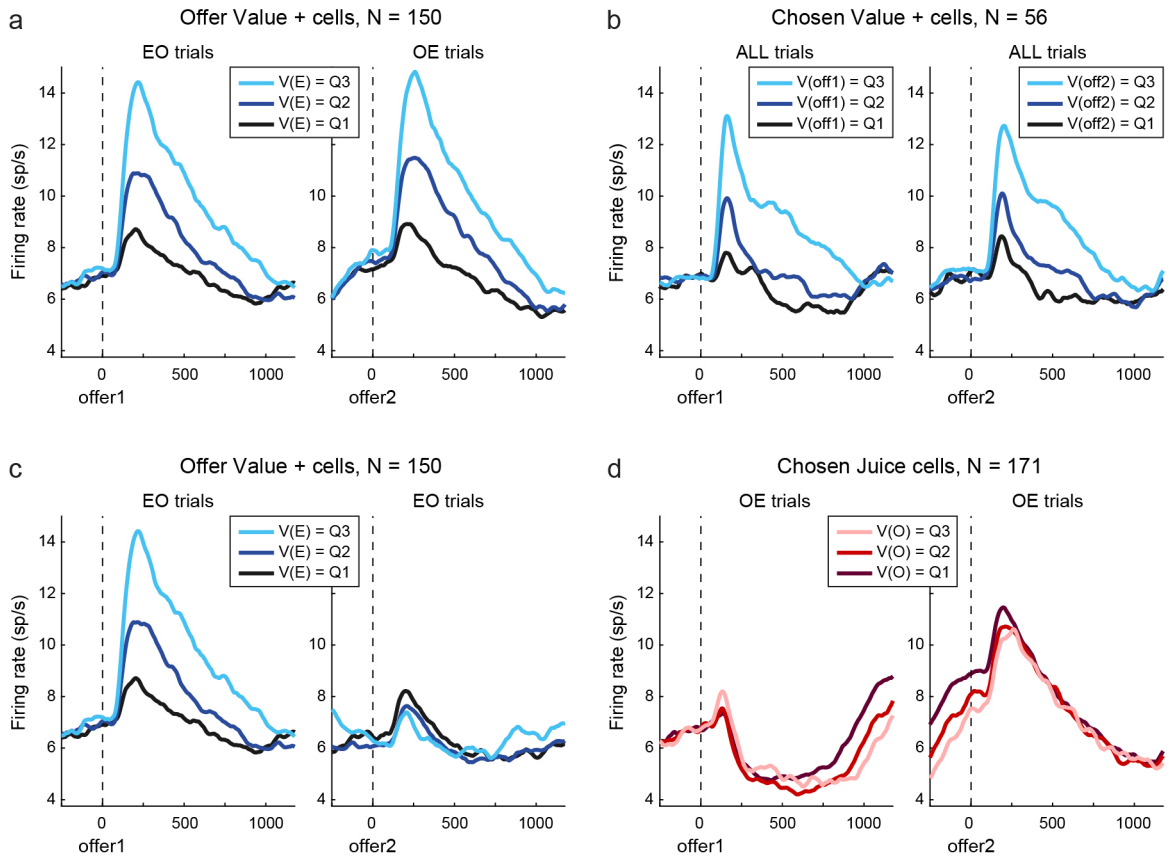

Figure 6. Activity profiles and decision mechanisms. **(a)** Lack of mutual inhibition in offer value cells. For each cell, "E" and "O" are the encoded juice and the other juice, respectively. V(E) and V(O) are the value of juice E and the value of juice O, respectively. Left and right panels show the firing rates in EO trials during offer1 and the firing rates in OE trials during offer2, respectively. (Hence, both panels illustrate the activity upon presentation of juice E.) For each cell, we divided trials in three groups corresponding to low, medium and high values of V(E) (Q1,Q2,Q3 are tertiles of the distribution for V(E)). We computed the three activity profiles and averaged them across the population. If decisions relied on mutual inhibition between pools of offer value cells, activity profiles in the right panel should be substantially lower compared to the left panel (because of inhibition taking place upon offer2, but not upon offer1). In contrast, the two sets of activity profiles were nearly identical. **(b)** Lack of mutual inhibition in chosen value cells. Here we pooled trials with different presentation order. In each panel, we divided trials in three groups according to the value offered in the corresponding time window (V(off1) in the left panel, V(off2) in the right panel). Again, the two sets of activity profiles were nearly identical. **(c)** Lack of working memory signal in offer value cells. Here we focused on EO trials and we divided trials according to V(E). The left panel is as in panel a. The right panel shows the same activity traces later in the trial, upon offer2. If decisions relied on a sustained working memory signal encoding the value of offer1 until offer2 presentation, traces in the right panel should be separated. The data belie this prediction. **(d)** Negative offset in chosen juice cells. Both panels illustrate the activity in OE trials. Trials were divided in three groups according to V(O) (i.e., the value of offer1). Over the course of the delay between the two offers, chosen juice cells developed a signal negatively related to V(O). This signal set a negative offset on the activity elicited by offer2 (right panel).

neurons best explained by the variable *value diff (A-B)* in the post-offer2 time window were vanishingly few (<1%; **Fig.4b**). Further analysis of the activity profiles confirmed this point. For each *offer value* cell, we labeled the encoded juice as "E" and the other juice as "O". We thus refer to EO trials and OE trials depending on whether juice E was offered first or second. (This convention made it possible to pool *offer value A* cells and *offer value B* cells.) We divided trials in three groups depending on whether the value of juice E was low, medium or high. According to H3, the responses of *offer value* cells to juice E should be reduced when juice E is presented as offer2 compared to when juice E is presented as offer1 (due to inhibition). In contrast to this prediction, responses recorded after offer1 (EO trials) and after offer2 (OE trials) were nearly identical (**Fig.6a**). A similar analysis conducted on *chosen value* cells provided similar results (**Fig.6b**). In conclusion, our data did not support the hypothesis of mutual inhibition at the level of offer values.

Hypothesis 4: Working memory activity in offer value cells. Under H1, H2 or H3, the neural mechanisms underlying decisions under sequential offers would be fundamentally different from those underlying decisions under simultaneous offers. The alternative possibility is that decisions in the two modalities are formed in the same neural circuit. When offers are sequential, the brain must maintain information about the first offer value and eventually use it in the decision process. Current models for choices under simultaneous offers (**Fig.1ab**) lack this function and thus do not support choices under sequential offers. However, these models could be adapted to do so. Consider the situation in which offers are sequential and good A is offered first. One reasonable hypothesis is that the pool of *offer value A* cells has some mechanism of working memory. If so, these neurons could maintain a sustained activity throughout the delay intervening between offer1 and offer2. After offer2, the decision would unfold as if the two offers were presented simultaneously. To evaluate this hypothesis, we focused on *offer value* cells and examined EO trials in both post-offer1 and post-offer2 time windows. Contrary to the prediction, we did not find any sustained activity encoding the value of offer1 (**Fig.6c**). An analysis of *chosen value* cells provided similar results (**Fig.S2**). Thus the memory trace of offer1 is not maintained through the sustained activity of *offer value* cells in OFC. In principle, this memory trace could be kept at the synaptic level or outside of OFC (see Discussion).

Hypothesis 5: Circuit inhibition. Aside from the mechanisms of working memory maintenance, we inquired how the value of offer1 might enter the decision process. Our data suggested a mechanism of circuit inhibition whereby *offer value* cells associated with one juice indirectly inhibit *chosen juice* cells associated with the other juice. **Fig.6d** illustrates the critical finding. In this analysis, we focused on *chosen juice* cells. For each neuron, the juice eliciting higher (lower) firing rates was labeled as juice E (juice O). We examined OE trials, and we divided trials according to the value of the first offer (i.e., the value of juice O). The activity of *chosen juice* cells increased shortly after offer1, and then dropped. However, over the course of the delay intervening between the two offers, the activity gradually increased and became *negatively* modulated by the value of offer1. At the time of offer2, the firing rates of *chosen juice* cells had a strong offset negatively related to the value of the other, non-encoded juice.

This observation may be interpreted in relation to the network depicted in **Fig.1a**. In the model, *offer value* cells and *chosen juice* cells are, respectively, the input and the output layers of the decision circuit. The decision is a competition between attractor states of *chosen juice* cells, mediated by *chosen value* cells. This competition is informed by the input of *offer value* cells and by the initial condition of the network[18,34]. Now consider trials in which juice A is offered first. The activity of *chosen juice B* cells immediately before offer2 represents the network's initial condition. Our results indicate that *offer value A* cells indirectly inhibit *chosen juice B* cells

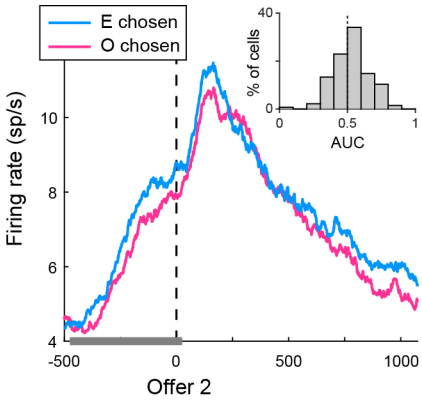

Figure 7. Choice probability in chosen juice cells. We examined the activity of chosen juice cells in OE trials upon presentation of offer2 (i.e., presentation of juice E). We specifically focused on offer types for which the animals split its decision. For each cell and each offer type, we divided trials according to the chosen juice (E or O), and we computed the two activity profiles. We also conducted the ROC analysis and obtained the AUC. We then averaged the activity profiles across trial types and across neurons. The traces showns here were obtained from 135 cells for which we could compute both activity profiles. The insert shows the distribution of AUC across the population (Methods). The distribution was significantly displaced from chance (mean(AUC)=0.53; p=0.029, paired t-test). In other words, stochastic fluctuations in the activity offset of chosen juice cells prior to offer2, corresponding to the initial conditions of the dynamic network, were significaintly correlated with the choice outcome.

(**Fig.6d**). By setting a negative offset on the network's initial condition, this inhibition imposes a bias against juice B (i.e., in favor of juice A) proportional to the offer value A. The phenomenon illustrated in **Fig.6d** is reminiscent of the predictive activity observed in a previous study[13] and reproduced by the same network[18]. In the previous study, the two juices were offered simultaneously, and the initial condition of the neural assembly, set by the outcome of the previous trial, imposed a bias in favor of repeating the same choice (choice hysteresis)[13]. Here, the neural circuit makes a decision only after offer2, and the initial condition is set by offer1.

In our interpretation, the activity offset of *chosen juice* cells immediately before offer2 captures the initial condition of the decision circuit. If so, stochastic fluctuations in this activity offset should be a source of choice variability[8]. To test this prediction, we examined *chosen juice* cells in OE trials. For each neuron, we identified offer types for which the animal split choices. Focusing on the 0.5 s preceding offer2, we divided trials according to the chosen juice (E or O), and we compared the two distributions of firing rates with an ROC analysis. The analysis returned an area under the curve (AUC), also termed choice probability. Importantly, our measure of choice probability quantified the correlation between activity offset and choices above and beyond that imposed by different values of offer1 (see Methods). Across the population, choice probabilities were significantly above chance (mean AUC = 0.525, p = 0.029, paired t-test; **Fig.7**). In other words, all other things equal, trial-by-trial fluctuations in the offset of *chosen juice* cells were significantly correlated with fluctuations in choice.

Discussion

A unitary account for economic decisions

There is a broad consensus that binary choices between goods are formed in the OFC[8,35-38], but current notions were almost exclusively derived from studies where two offers were presented simultaneously. Yet, in many real-life decisions, offers appear (or are examined) sequentially. At first, the distinction between choices under simultaneous and sequential offers might seem negligible. However, computational models for the former[17-21] do not account for the latter, and previous studies that focused on choices under sequential offers suggested that fundamentally different mechanism underlie decisions in the two modalities[24,30-32]. Revisiting this pivotal question, we examined the activity of neurons in OFC using a choice task and data analyses comparable to those previously used for choices under simultaneous offers[15,16]. Neuronal

responses recorded in any given time window often depended on the presentation order. However, an analysis across time windows revealed the presence of a small number of cell groups seemingly analogous to the groups of cells previously identified under simultaneous offers[12,13]. Additional work is necessary to confirm this correspondence. With this caveat, our findings suggest that decisions in the two modalities are formed in the same neural circuit. Building on this result, we tested several hypotheses on the decision mechanisms. Our data clearly argue against the notion of a single pool of neurons[30]. Contrary to previous assessments, our data also argue against the idea that decisions are made through mutual inhibition between pools of *offer value* cells. In principle, decisions under sequential offers could rely on sustained working-memory activity in the neuronal pool representing the first offer value, but our data do not support this hypothesis. Conversely, our data suggest that *offer value* cells associated with the first offer indirectly inhibit *chosen juice* cells associated with the second offer – a phenomenon referred to as circuit inhibition.

The idea that the same neural circuit underlies decisions under both simultaneous and sequential offers stands to reason. Two dedicated circuits might seem wasteful. Furthermore, the line between the two modalities is often blurred, because goods presented simultaneously may be examined in sequence. Still, it is worth reflecting on the advantages of circuit inhibition compared to other decision mechanisms discussed here. First, the concept of non-binary accept/reject decisions may be partly misconstrued. Indeed, an accept/reject decision is always a binary choice between some option and aspects of the status quo – often in the form of opportunities – that would be lost if that option were chosen. Future research should examine the neural mechanisms of accept/reject decisions in this perspective. Second, under mutual inhibition, neurons encoding the two offer values inhibit each other. As a result, each pool of neurons comes to encode the value difference, or perhaps the maximum between the value difference and zero. From a computational perspective, one drawback of this putative mechanism is that decisions through the calculation of value differences generalize poorly to choices between multiple options. Indeed, the number of differences to be computed increases exponentially with the number of options, and this large number of operations still does not resolve the decision. In contrast, the dynamic system depicted in **Fig.1a** generalizes naturally to choices between multiple items[39,40].

The model in **Fig.1a** appears to lack two important functions. First, under sequential offers, the brain must keep track of the first offer value throughout a delay. Inspection of **Fig.6** suggests that this working memory might be kept at the synaptic level[41,42], or perhaps outside of the decision circuit. Second, upon offer1, *chosen juice* cells respond in a binary way to the offered juice. In itself, this signal is similar to that reflecting the binary choice outcome after the decision. Thus there must be some breaking mechanism preventing the animal from finalizing its choice. One possibility is that this breaking function involves the lateral prefrontal cortex (LPFC), which is densely interconnected with OFC[43,44]. Indeed, previous work indicated LPFC as a key node in the transition from the decision circuit to motor circuits, where choices are implemented[45]. Future research should investigate these important issues.

Implications for choices under free viewing

Although this was cast as a study of decisions under sequential offers, the results also shed light on another fundamental issue, namely the role played by attention or mental focus in economic decisions. It was often noted that neurons in the primate OFC are not spatially selective[12,46]. At the same time, recent studies showed that neurons in this area can be modulated by gaze or attentional shifts[47,48]. Our results corroborate both of these observations,

as many neurons encoded the value of a particular juice, but only when that juice was present on the monitor. In our task, animals maintained center fixation while offers appeared and disappeared centrally on the monitor. Thus our results indicate that neurons in OFC are modulated by shifts of mental focus, not by shifts of gaze direction per se. This understanding is also consistent with previous findings[47-49].

From the perspective of the choice system, situations in which subjects shift their gaze or the attention spotlight back and forth between two options on display are presumably similar to the situation examined here, where the gaze is fixed and two options appear foveally in turn. If so, one might speculate about the neuronal mechanisms underlying decisions in the former case. Our results suggest that, upon each gaze shift, OFC neurons encoding the value of the currently attended offer indirectly inhibit the activity of cells representing the opposite choice outcome. Future studies should test this prediction. If confirmed, this understanding would reconcile seemingly diverging ideas put forth in recent years[8,49,50].

Methods

Experimental design, surgery and recordings

All experimental procedures conformed to the NIH *Guide for the Care and Use of Laboratory Animals* and were approved by the Institutional Animal Care and Use Committee (IACUC) at Washington University. Two male rhesus monkeys participated in the study (G: age 6, 9.6 kg; J: age 7, 10.1 kg). The animals sat in an electrically insulated enclosure with their head restrained. A computer monitor was placed 57 cm in front the animal. The behavioral task was controlled through custom-written software (http://www.monkeylogic.net/). The gaze direction was monitored by an infrared video camera (Eyelink; SR Research) at 1 kHz, with an estimated spatial resolution of 0.2°.

In each session, the animal chose between two juices labeled A and B, with A preferred. The two juices were offered sequentially and in variable amounts. **Fig.2** illustrates the task design. Each trial began with the animal fixating a dot (0.35° of visual angle) in the center of the monitor. After 0.5 s, two offers appeared centrally and sequentially. Each offer was represented by a set of colored squares, where the color indicated the juice type and the number of squares indicated the juice amount. For example, in the trial depicted in **Fig.2a**, the animal chose between two drops of grape juice and six drops of peppermint tea. Along with the offer, a small colored circle (0.75° of visual angle) appeared around the fixation dot. In the case of null offer (0 drops), the circle indicated to the animal the identity of the corresponding juice. The animal maintained center fixation throughout the initial fixation (0.5 s), offer1 time (0.7 s), inter-offer time (0.5 s), offer2 time (0.7 s), wait time (0.5 s), and delay time (0.5-1 s). At the end of the delay, the fixation point was extinguished. The animal indicated its choice with a saccade and maintained peripheral fixation for 0.6 s before juice delivery. Center fixation was imposed with a tolerance 2.5°. In a subset of sessions (37%), offer2 was presented for 0.5 s. Sessions included 300-800 trials and offered quantities varied from trial to trial pseudo-randomly (**Fig.2b**). For each pair of juice quantities, the presentation order (AB, BA) and the spatial location of the saccade targets varied pseudo-randomly and were counterbalanced across trials. Across sessions, we used 12 different juices, resulting in a large number of juice pairings. The association between juice type and color remained fixed throughout the experiments. The juice quantum (i.e., the volume of one drop) was set between 70 µl and 100 µl of volume and did not change during a given session. Importantly, both animals were initially naive. Both of them were trained directly with sequential offers, without previous exposure to the standard choice task (simultaneous offers)[12].

In each animal, we implanted a head-restraining device and an oval recording chamber (Crist Instruments) under general anesthesia. The chamber (main axes, 50 X 30 mm) was centered on stereotaxic coordinates (A30, L0), with the longer axis parallel to a coronal plane. Recordings were obtained from individual neurons in the central orbital gyrus of both hemispheres using tungsten electrodes (100 µm shank diameter; FHC) advanced with a custom-made motorized system driven remotely. Electrodes were typically advanced in pairs (one motor for two electrodes), with the two electrodes placed at 1 mm from each other. Electric signals were amplified (gain 10,000), filtered (high-pass cutoff, 300 Hz; low-pass cutoff, 6 kHz; Lynx 8; Neuralynx) and recorded (Power 1401; Cambridge Electronic Design). Action potentials were detected on-line and waveforms (40 kHz sampling rate) were saved to disk for off-line clustering (Spike 2; Cambridge Electronic Design). Only cells that appeared well isolated and stable throughout the session were included in the analysis. The data set thus included 829 cells from monkey G and 438 cells from monkey J, recorded over the course of 209 sessions.

Analysis of choice patterns

All the analyses were conducted in Matlab (MathWorks Inc). Labels "AB" and "BA" indicate the presentation offer (in AB trials A is offered first). Choice patterns were analyzed with a logistic regression

$$\text{choice B} = 1/(1+\exp(-X))$$
$$X = a_0 + a_1 \log(q_B/q_A) + a_2 (\delta_{order,AB} - \delta_{order,BA}) \quad (3)$$

where q_A and q_B are the quantities of juices A and B offered to the animal, $\delta_{order,AB} = 1$ in AB trials and 0 in BA trials, and $\delta_{order,BA} = 1 - \delta_{order,AB}$. From the fitted parameters, we derived measures for the relative value of the juices (ρ), the sigmoid steepness (η) and the order bias (ε), defined as follows:

$$\rho = \exp(-a_0 / a_1) \quad (4)$$
$$\eta = a_1$$
$$\varepsilon = \exp(-a_2 / a_1)$$

Both animals presented an appreciable order bias favoring offer2 (monkey G: mean(ε) = 0.10, $p<0.001$; monkey J: mean(ε) = 0.31, $p<0.001$). However, the order bias was typically small compared to the relative value (monkey G: mean(ρ) = 2.5; monkey J: mean(ρ) = 3.8). Thus the variables examined in the analysis of neuronal data, were defined based on ρ, independent of ε (see below).

Cell classification

Procedures for the analysis of neuronal data were similar to those previously used in studies of choices under simultaneous offers[12,13]. Each cell was analyzed in relation to the choice pattern recorded in the same session. We defined several 0.5 s time windows aligned with different behavioral events: pre-offer (0.5 s before offer1; a control time window), post-offer1 (0.1-0.6 s after offer1), inter-offer (from 0.4 s before to 0.1 s after offer2), post-offer2 (from 0.1-0.6 s after offer2), offers off (0.6-1.1 s after offer2), fixation off (from 0.1 s before to 0.4 s after extinction of the center fixation point), pre-juice (from 0.4 s before to 0.1 s after juice delivery onset) and post-juice (0.1-0.6 s after juice delivery onset). An "offer type" was defined by two juice quantities in given order (e.g., [1A:3B] or [3B:1A]); a "trial type" was defined by an offer type and a choice (e.g., [1A:3B, B]); and a "neuronal response" was defined as the activity of one cell in one time window as a function of the trial type.

The analysis proceeded in steps. First, data underwent an ANOVA (factor: trial type). Neurons that passed the significance threshold ($p<0.001$) in at least one time window were identified as "task-related" and included in subsequent analyses. Second, we defined a large number of variables that neurons in the OFC could conceivably encode. These included one binary variable representing the order (*AB* | *BA*), eight variables representing individual offer values (*offer value A*, *offer value A* | *AB*, *offer value A* | *BA*, *offer value B*, *offer value B* | *AB*, *offer value B* | *BA*, *offer value 1*, *offer value 2*), variables representing the binary choice outcome (*chosen juice*, *chosen order*), variables capturing variants of the chosen value (*chosen value*, *chosen value A*, *chosen value B*) and variables capturing the value difference (*value diff (ch–oth)*; *value diff (A–B)*; *value diff (1–2)*). The 18 variables included in the analysis are defined in **Table S2**. Each response passing the ANOVA criterion was regressed on each variable. A variable was said to "explain" the response if the regression slope differed significantly from zero ($p<0.05$). In

this case, we noted the sign of the encoding (regression slope >0 or <0). Each linear regression also provided an R^2. When a response was explained by more than one variable, the variable with the largest R^2 was said to provide the best fit for the response. For variables that did not explain the response, we set R^2=0.

Neurons often encoded different variables in different time windows. However, preliminary observations of neuronal responses across time windows suggested that a small number of variable sequences could account for a large fraction of the population. We thus set up to examine neurons across multiple time windows. Specifically, we focused on the three time windows post-offer1, post-offer2 and post-juice. In this analysis, we used signed variables, where the sign was that obtained from the regression slope. Given 36 signed variables and 3 time windows, there were 46,656 possible sequences. To identify a small number sequences that can best account for the neuronal population, one would ideally run an exhaustive analysis of all the subsets of k sequences, with k = 1,2,3... However, the large number of possible sequences made this approach computationally unfeasible. To reduce the number of possible sequences, we proceeded as follows. First, for each neuron and for each sequence, we defined the "sequence R^2" as the sum(R^2) across time windows. A sequence was said to "explain" a cell if the sequence R^2 was >0. For each neuron, we identified the sequence that provided the best explanation (highest sequence R^2). Second, we noted that a relatively small number of sequences (N=387) provided the best explanation for ≥1 cell. Considering sequences providing the best explanation for ≥3 cells along with their mirror sequences (obtained by flipping the encoding signs) further reduced this number to N=26 (see **Table S3**). We thus focused on these sequences, and proceeded with an exhaustive analysis. For k = 1,2,3... we examined each subset of k sequences (>5 × 10^6 possible subsets). For each subset, we computed the total R^2 by assigning each neuron to the best sequence in the subset and by summing the sequence R^2 across all cells. For k = 1,2,3... we thus identified the best subset as that providing the maximum total R^2. (Time windows that did not pass the ANOVA and variables that did not explain a response were normally not considered in these computations. However, these time windows were used to disambiguate cases in which two sequences provided the same sequence R^2.)

Once identified the best subset of 8 sequences, we assigned each neuron to the sequence providing the highest sequence R^2 (**Table 1**).

Analysis of activity profiles

Having identified different groups of neurons, we proceeded with the analysis of their activity profiles. For each *offer value* cell and for each *chosen juice* cell, we labeled the encoded juice as "E" and the other juice as "O". (For *chosen juice* cells, the encoded juice was that eliciting higher firing rates.) For each cell, we thus refer to EO trials and OE trials depending on whether juice E was offered first or second. These conventions made it possible to pool neurons associated with different juices (A or B). Since we wanted to focus on trials in which the animal could not finalize its decision prior to offer2, we removed from the analysis all forced choices (i.e., trials in which one of the offers was 0). For symmetry, we excluded forced choices independently of whether the null offer was offer1 or offer2. To calculate activity profiles, trials were separately aligned at the times of offer1 and offer2. For each trial, the spike train was smoothed using a kernel that mimicked the post-synaptic potential by exerting influence only forward in time (decay time constant = 20 ms)[51]. **Fig.7** and **Fig.S2** were generated with no additional smoothing. For display purposes, we used a moving average of 50 ms in **Fig.6**. For several analyses, we computed the activity profile of a particular population dividing trials in tertiles according to some variable. For example in **Fig.6a**, we examined *offer value* cells in EO

trials and divided trials according to the offer value E (V(E)). To do so, the distribution of V(E) was divided in tertiles for each neuron, and the three activity profiles were averaged across the population.

The activity of *chosen juice* cells was examined with a receiver operating characteristic (ROC) analysis[52,53]. This analysis was performed on a 500 ms time window starting 475 ms before offer2. The ROC analysis was conducted on raw spike counts, without time averaging or baseline correction. We focused on offer types for which the animal split its choices between the two juices, and we excluded trial types with <4 trials. For each offer type, we divided trials depending on the chosen juice (E or O) and we compared the two distributions. The ROC analysis provided an area under the curve (AUC), also termed choice probability[52,53]. To obtain a single AUC for each neuron, we averaged the AUC across offer types[54]. Importantly, this measure quantified the correlation between variability in firing rates and variability in choices above and beyond the correlation imposed by the value of offer1.

References

1. Rahman, S., Sahakian, B.J., Hodges, J.R., Rogers, R.D. & Robbins, T.W. Specific cognitive deficits in mild frontal variant of frontotemporal dementia. *Brain* **122 (Pt 8)**, 1469-1493 (1999).
2. Volkow, N.D. & Li, T.K. Drug addiction: the neurobiology of behaviour gone awry. *Nat Rev Neurosci* **5**, 963-970 (2004).
3. Heyman, G.M. *Addiction: a disorder of choice*, (Harvard University Press, Cambridge, MA, 2009).
4. Bartra, O., McGuire, J.T. & Kable, J.W. The valuation system: a coordinate-based meta-analysis of BOLD fMRI experiments examining neural correlates of subjective value. *Neuroimage* **76**, 412-427 (2013).
5. Clithero, J.A. & Rangel, A. Informatic parcellation of the network involved in the computation of subjective value. *Soc Cogn Affect Neurosci* (2013).
6. Wallis, J.D. Cross-species studies of orbitofrontal cortex and value-based decision-making. *Nat Neurosci* **15**, 13-19 (2012).
7. Rudebeck, P.H. & Murray, E.A. The orbitofrontal oracle: cortical mechanisms for the prediction and evaluation of specific behavioral outcomes. *Neuron* **84**, 1143-1156 (2014).
8. Padoa-Schioppa, C. & Conen, K.E. Orbitofrontal cortex: A neural circuit for economic decisions. *Neuron* **96**, 736-754 (2017).
9. Gallagher, M., McMahan, R.W. & Schoenbaum, G. Orbitofrontal cortex and representation of incentive value in associative learning. *J Neurosci* **19**, 6610-6614 (1999).
10. Camille, N., Griffiths, C.A., Vo, K., Fellows, L.K. & Kable, J.W. Ventromedial frontal lobe damage disrupts value maximization in humans. *J Neurosci* **31**, 7527-7532 (2011).
11. Rudebeck, P.H., Saunders, R.C., Prescott, A.T., Chau, L.S. & Murray, E.A. Prefrontal mechanisms of behavioral flexibility, emotion regulation and value updating. *Nat Neurosci* **16**, 1140-1145 (2013).
12. Padoa-Schioppa, C. & Assad, J.A. Neurons in orbitofrontal cortex encode economic value. *Nature* **441**, 223-226 (2006).
13. Padoa-Schioppa, C. Neuronal origins of choice variability in economic decisions. *Neuron* **80**, 1322-1336 (2013).
14. Xie, J. & Padoa-Schioppa, C. Neuronal remapping and circuit persistence in economic decisions. *Nat Neurosci* **19**, 855-861 (2016).
15. Conen, K.E. & Padoa-Schioppa, C. Neuronal variability in orbitofrontal cortex during economic decisions. *J Neurophysiol* **114**, 1367-1381 (2015).
16. Rich, E.L. & Wallis, J.D. Decoding subjective decisions from orbitofrontal cortex. *Nat Neurosci* **19**, 973-980 (2016).
17. Solway, A. & Botvinick, M.M. Goal-directed decision making as probabilistic inference: a computational framework and potential neural correlates. *Psychological Review* **119**, 120-154 (2012).
18. Rustichini, A. & Padoa-Schioppa, C. A neuro-computational model of economic decisions. *J Neurophysiol* **114**, 1382-1398 (2015).
19. Friedrich, J. & Lengyel, M. Goal-directed decision making with spiking neurons. *J Neurosci* **36**, 1529-1546 (2016).
20. Song, H.F., Yang, G.R. & Wang, X.J. Reward-based training of recurrent neural networks for cognitive and value-based tasks. in *Elife*, Vol. 6 (2017).
21. Zhang, Z., Cheng, Z., Lin, Z., Nie, C. & Yang, T. A neural network model for the orbitofrontal cortex and task space acquisition during reinforcement learning. *PLoS Comput Biol* **14**, e1005925 (2018).

22. Wallis, J.D. & Miller, E.K. Neuronal activity in primate dorsolateral and orbital prefrontal cortex during performance of a reward preference task. *Eur J Neurosci* **18**, 2069-2081 (2003).
23. Strait, C.E., Blanchard, T.C. & Hayden, B.Y. Reward value comparison via mutual inhibition in ventromedial prefrontal cortex. *Neuron* **82**, 1357-1366 (2014).
24. Strait, C.E., Sleezer, B.J. & Hayden, B.Y. Signatures of value comparison in ventral striatum neurons. *PLoS Biol* **13**, e1002173 (2015).
25. Blanchard, T.C., Hayden, B.Y. & Bromberg-Martin, E.S. Orbitofrontal cortex uses distinct codes for different choice attributes in decisions motivated by curiosity. *Neuron* **85**, 602-614 (2015).
26. Azab, H. & Hayden, B.Y. Correlates of decisional dynamics in the dorsal anterior cingulate cortex. *PLoS Biol* **15**, e2003091 (2017).
27. Azab, H. & Hayden, B.Y. Correlates of economic decisions in the dorsal and subgenual anterior cingulate cortices. *Eur J Neurosci* **47**, 979-993 (2018).
28. Blanchard, T.C., Piantadosi, S. & Hayden, B.Y. Robust mixture modeling reveals category-free selectivity in reward region neuronal ensembles. *J Neurophysiol*, jn 00808 02017 (2017).
29. Hunt, L.T.*, et al.* Triple dissociation of attention and decision computations across prefrontal cortex. *Nat Neurosci* **21**, 1471-1481 (2018).
30. Hayden, B.Y. & Moreno-Bote, R. A neuronal theory of sequential economic choice. *Brain and Neuroscience Advances*, 1-15 (2018).
31. Kacelnik, A., Vasconcelos, M. & Monteiro, T. Darwin's "tug-of-war" vs. starling's "horse-racing": how adaptations for sequential encounters drive simultaneous choice. *Behav Ecol Sociobiol* **65**, 547-558 (2011).
32. Hunt, L.T., Woolrich, M.W., Rushworth, M.F. & Behrens, T.E. Trial-type dependent frames of reference for value comparison. *PLoS Comput Biol* **9**, e1003225 (2013).
33. Raghuraman, A.P. & Padoa-Schioppa, C. Integration of multiple determinants in the neuronal computation of economic values. *J Neurosci* **34**, 11583-11603 (2014).
34. Wang, X.J. Probabilistic decision making by slow reverberation in cortical circuits. *Neuron* **36**, 955-968 (2002).
35. Cisek, P. Making decisions through a distributed consensus. *Curr Opin Neurobiol* **22**, 927-936 (2012).
36. Rushworth, M.F., Kolling, N., Sallet, J. & Mars, R.B. Valuation and decision-making in frontal cortex: one or many serial or parallel systems? *Curr Opin Neurobiol* **22**, 946-955 (2012).
37. Wunderlich, K., Rangel, A. & O'Doherty, J.P. Economic choices can be made using only stimulus values. *Proc Natl Acad Sci U S A* **107**, 15005-15010 (2010).
38. Rudebeck, P.H. & Rich, E.L. Orbitofrontal cortex. *Current Biology* **28**, R1083-R1088 (2018).
39. Furman, M. & Wang, X.J. Similarity effect and optimal control of multiple-choice decision making. *Neuron* **60**, 1153-1168 (2008).
40. Wang, X.J. Neural dynamics and circuit mechanisms of decision-making. *Current Opinion in Neurobiology* **22**, 1039-1046 (2012).
41. Mongillo, G., Barak, O. & Tsodyks, M. Synaptic theory of working memory. *Science* **319**, 1543-1546 (2008).
42. Stokes, M.G. 'Activity-silent' working memory in prefrontal cortex: a dynamic coding framework. *Trends Cogn Sci* **19**, 394-405 (2015).
43. Petrides, M. & Pandya, D.N. Efferent association pathways originating in the caudal prefrontal cortex in the macaque monkey. *J Comp Neurol* **498**, 227-251 (2006).
44. Saleem, K.S., Miller, B. & Price, J.L. Subdivisions and connectional networks of the lateral prefrontal cortex in the macaque monkey. *J Comp Neurol* (2013).

45. Cai, X. & Padoa-Schioppa, C. Contributions of orbitofrontal and lateral prefrontal cortices to economic choice and the good-to-action transformation. *Neuron* **81**, 1140-1151 (2014).
46. Grattan, L.E. & Glimcher, P.W. Absence of spatial tuning in the orbitofrontal cortex. *PLoS One* **9**, e112750 (2014).
47. McGinty, V.B., Rangel, A. & Newsome, W.T. Orbitofrontal cortex value signals depend on fixation location during free viewing. *Neuron* **90**, 1299-1311 (2016).
48. Xie, Y., Nie, C. & Yang, T. Covert shift of attention modulates the value encoding in the orbitofrontal cortex. *Elife* **7**(2018).
49. Krajbich, I., Armel, C. & Rangel, A. Visual fixations and the computation and comparison of value in simple choice. *Nat Neurosci* **13**, 1292-1298 (2010).
50. Hare, T.A., Schultz, W., Camerer, C.F., O'Doherty, J.P. & Rangel, A. Transformation of stimulus value signals into motor commands during simple choice. *P Natl Acad Sci USA* **108**, 18120-18125 (2011).
51. So, N.Y. & Stuphorn, V. Supplementary eye field encodes option and action value for saccades with variable reward. *J Neurophysiol* **104**, 2634-2653 (2010).
52. Britten, K.H., Shadlen, M.N., Newsome, W.T. & Movshon, J.A. The analysis of visual motion: a comparison of neuronal and psychophysical performance. *J Neurosci* **12**, 4745-4765 (1992).
53. Green, D.M. & Swets, J.A. *Signal detection theory and psychophysics*, (Wiley, New York,, 1966).
54. Kang, I. & Maunsell, J.H. Potential confounds in estimating trial-to-trial correlations between neuronal response and behavior using choice probabilities. *J Neurophysiol* **108**, 3403-3415 (2012).